45 Toh Y, Yamamoto M, Endo H, Misumi Y, Ikehara Y. Isolation and characterization of a rat liver alkaline phosphatase gene. A single gene with two promoters. *Eur J Biochem* 1989; **182**: 231–7.
46 Alpers DH, Eliakim R, DeSchryver-Kecskemeti K. Secretion of hepatic and intestinal alkaline phosphatases: similarities and differences. *Clin Chim Acta* 1990; **186**: 211–23.
47 Yusifov TN, Abduragimov AR, Gasymov OK, Glasgow BJ. Endonuclease activity in lipocalins. *Biochem J* 2000; **347**: 815–19.
48 Pan CQ, Lazarus. RA. Hyperactivity of human DNase I variants. Dependence on the number of positively charged residues and concentration, length, and environment of DNA. *J Biol Chem* 1998; **273**: 11701–8.
49 Fraga CG, Shigenaga MK, Park JW, Degan P, Ames BN. Oxidative damage to DNA during aging. 8-hydroxy-2′-deoxyguanosine in rat organ DNA and urine. *Proc Natl Acad Sci USA* 1990; **87**: 4533–7.
50 Tchou J, Bodepudi V, Shibutani S, Antoshechkin I, Miller J, Grollman AP, Johnson F. Substrate specificity of Fpg protein. Recognition and cleavage of oxidatively damaged DNA. *J Biol Chem* 1994; **269**: 15318–24.
51 David SS, Williams SD. Chemistry of glycosylases and endonucleases involved in base-excision repair. *Chem Rev* 1998; **98**: 1221–62.
52 Weimann A, Riis B, Poulsen HE. Oligonucleotides in human urine do not contain 8-oxo-7,8-dihydrodeoxyguanosine. *Free Radic Biol Med* 2004; **36**: 1378–82.

 doi: 10.1111/j.1349-7006.2005.00004.x

Available online at www.sciencedirect.com
SCIENCE DIRECT®
Mutation Research 572 (2005) 132–141
Fundamental and Molecular Mechanisms of Mutagenesis
www.elsevier.com/locate/molmut
Community address: www.elsevier.com/locate/mutres

Frequent retention of heterozygosity for point mutations in *p53* and *Ikaros* in *N*-ethyl-*N*-nitrosourea-induced mouse thymic lymphomas

Shizuko Kakinuma [a,*], Mayumi Nishimura [a], Ayumi Kubo [a], Jun-ya Nagai [a], Yoshiko Amasaki [a], Hideyuki J. Majima [b], Toshihiko Sado [a], Yoshiya Shimada [a,**]

[a] *Low Dose Radiation Effect Research Project, National Institute of Radiological Sciences, Chiba, Japan*
[b] *Department of Oncology, Division of Maxillofacial Radiology and Department of Space Environmental Medicine, Graduate School of Medical and Dental Sciences, Kagoshima University, Kagoshima, Japan*

Received 19 September 2004; received in revised form 29 December 2004; accepted 7 January 2005

Abstract

In agreement with Knudson's two-hit theory, recent findings indicate that the inactivation of tumor suppressor genes is not only mediated by the loss of function but also by the dominant-negative or gain-of-function activity. The former generally accompanies loss of a wild-type allele whereas in the latter a wild-type allele is retained. *N*-Ethyl-*N*-nitrosourea (ENU), which efficiently induces point mutations, reportedly leads to the development of tumors by activating *ras* oncogenes. Little is known about how ENU affects tumor suppressor genes and, therefore, we examined ENU-induced mutations of *p53* and *Ikaros* in thymic lymphomas and compared these with mutations of K*ras*. In addition, loss of heterozygosity was examined for chromosome 11 to which both *p53* and *Ikaros* were mapped. The frequency of point mutations in *p53* and *Ikaros* was 30% (8/27) and 19% (5/27), respectively, comparable to that observed in K*ras* (33%: 9/27). In total, 14 of the 27 thymic lymphomas examined (52%) harbored mutations in at least one of these genes. One *Ikaros* mutation was located at the splice donor site, generating a novel splice isoform lacking zinc finger 3, *Ik (F3del)*. Interestingly, 90% (10/11) of the tumors with point mutations retained wild-type alleles of *p53* and *Ikaros*. Sequence analysis revealed that the most common nucleic acid substitutions were T > A (4/8) in *p53*, T > C (4/5) in *Ikaros* and G > A/T (8/9) in K*ras*, suggesting that the spectrum of mutations was gene dependent. These results suggest that point mutations in tumor suppressor genes without loss of the wild-type allele play an important role in ENU-induced lymphomagenesis.

Keywords: ENU; Heterozygous mutation; *p53*; *Ikaros*

1. Introduction

Tumor suppressor gene function can be inactivated either by point mutations or by deletion of both the alleles, known as Knudson's "two-hit" hypothesis [1,2]. In

* Corresponding author. Tel.: +81 34 206 3221; fax: +81 34 206 4138.
** Co-corresponding author.
E-mail addresses: skakinum@nirs.go.jp (S. Kakinuma), y_shimad@nirs.go.jp (Y. Shimada).

0027-5107/$ – see front matter © 2005 Elsevier B.V. All rights reserved.
doi:10.1016/j.mrfmmm.2005.01.010

an examination of colon cancers, Vogelstein and colleagues found that the most prevalent pattern of *p53* mutations was a point mutation in one allele concomitant with the loss of the other allele [3]. On the other hand, several lines of evidence suggest that given types of p53 act as oncogenes in a dominant manner in the presence of a wild-type allele [3,4]. Since p53 functions as a tetrameric transcription factor, mutant p53 lacking DNA-binding ability is thought to inhibit the function of wild-type p53 [5,6]. These lines of evidence indicate that negative dominancy adds a new perspective to our understanding of tumor suppressors. However, little data are available on oncogenic changes in other tumor suppressor genes.

Ikaros is a tumor suppressor gene for T and B cell leukemogenesis in both the mice and humans [7–10]. Ikaros is a Kruppel-type zinc finger transcription factor involved in lineage commitment and differentiation in the lymphoid cells. Heterozygous mice expressing a short Ikaros isoform lacking the DNA-binding zinc fingers show aberrant T cell differentiation and develop thymic lymphomas within 3 months after birth [11]. Biochemical analysis has revealed that Ikaros forms homodimers or heterodimers with other Ikaros family members such as Aiolos or Helios [12,13]. Thus, short Ikaros isoforms lacking DNA-binding domains function in a dominant-negative fashion against wild-type Ikaros. Similar to p53, one might predict that Ikaros mutants containing lesions in the DNA-binding domain would affect wild-type Ikaros in a dominant-negative manner. We previously demonstrated that short Ikaros isoforms lacking the DNA-binding domain are expressed in radiation-induced mouse thymic lymphomas [14,15]. These lymphomas frequently retain a wild-type allele, suggesting dominant-negative interactions. Point mutations of *Ikaros* were observed in other lymphomas that had lost a wild-type allele, consistent with Knudson's two-hit theory [14–17].

N-Ethyl-*N*-nitrosourea (ENU) is a hyper-mutable alkylating agent that efficiently induces point mutations [18,19]. Treatment of mice with ENU leads to a high incidence of thymic lymphoma. Mutation of K*ras* genes is more frequently observed in ENU-induced lymphomas than in radiation-induced lymphomas, suggesting that oncogene activation plays an important role in ENU-induced lymphomagenesis [20–23]. In contrast, a genome-wide survey of loss of heterozygosity (LOH) showed a significantly lower LOH rate in ENU-induced lymphomas than in radiation-induced lymphomas [14]. ENU also induces point mutations within the *Aprt* locus but these lesions do not occur by deletion/recombination [24,25]. Therefore, it is less likely that inactivation of tumor suppressor genes contributes to ENU-induced lymphomagenesis. As mentioned above, however, point mutations of *p53* without accompanying LOH have occasionally been reported [3].

The aim of this study was to examine the rate and spectrum of mutations in *Ikaros* and *p53* tumor suppressor genes associated with LOH and to determine the contribution of tumor suppressor genes to ENU-induced tumorigenesis. We found that the mutation rates of *Ikaros* and *p53* are comparable to that of K*ras* and that, in contrast to radiation-induced lymphomas, ENU-induced lymphomas retain a wild-type allele of these genes. Thus, we conclude that heterozygous point mutations of tumor suppressor genes significantly contribute to ENU-induced lymphomagenesis.

2. Materials and methods

2.1. Mice and tumor induction

B6C3F1 mice were purchased from Charles River, Kanagawa, Japan. Induction of thymic lymphomas by ENU (Nakali, Japan) was as described previously [26]. Briefly, thymic lymphomas were induced in female mice that were a cross between thymic lymphoma-susceptible C57BL/6 and thymic lymphoma-resistant C3H strains. Five-week-old mice received 400 ppm ENU in their drinking water for 8 weeks. Mice were observed daily until moribund after which they were sacrificed under ether anesthesia and autopsied. Thymic tissue was then removed, weighed and prepared for serological and molecular analyses [15]. All the animal experiments were conducted in compliance with the institutional guidelines for the care of laboratory animals.

2.2. Antibodies and immunofluorescence analysis

FITC-conjugated anti-CD8, anti-cKit, anti-CD44, and anti-TCR$\alpha\beta$, and PE-conjugated anti-CD4, anti-IL2, anti-CD3, and anti-TCR$\gamma\delta$ were purchased from Pharmingen (San Diego, CA). After dispersing

the thymus until single cells were obtained, 10^6 cells were resuspended in 50 μl PBS supplemented with 1% FBS and FITC and/or PE-conjugated antibodies at an optimal dilution for 30 min on ice. Control levels of fluorescence were determined after staining with the appropriate isotype-specific Igs. The relative fluorescence intensity of 10,000 cells in each sample was measured using FACScan and was analyzed with Cell Quest software (Becton Dickinson, Mountain View, CA).

2.3. Western blot analysis of p53 and Ikaros in thymocytes

Western blotting was performed as described previously [15] with the following minor modifications: after transfer of proteins from the gel, the membrane was blocked and probed with polyclonal antisera against p53 (1:5000; Santa Cruz Biotechnology Inc., Santa Cruz, CA) or Ikaros (1:5000). Blots were washed and then incubated with a peroxidase-conjugated goat anti-rabbit IgG secondary antibody (1:50,000; Amersham Pharmacia Biotech Inc., Piscataway, NJ). Ikaros proteins were detected using Super Signal Dura Chemiluminescent Substrate (Pierce, Rockford, IL) and were analyzed using a Kodak Digital analyzer (Kodak, Rochester, NY).

2.4. LOH analysis

Genomic DNA was extracted from the tumors according to the standard techniques. The LOH region on chromosome 11 was defined using the following 10 polymorphic loci: *D11Mit71*, *D11Mit62*, *D11Mit2*, *D11Mit204*, *D11Mit150*, *D11Mit77*, *D11Mit20*, *Acrb*, *D11Mit14* and *D11Mit203*. Single-strand length polymorphism (SSLP) analysis was performed as previously described [14].

2.5. Mutation analysis of Ikaros, p53 and Kras

Total RNA extracted from lymphoma cells was reverse-transcribed to obtain cDNA as described previously [15]. Expression status of *Ikaros* was determined using the primers *Ikaros* 2F and 7R and *Gapd* (sense and antisense) as a control. Mutations in the genes *p53*, *Ikaros* and K*ras* were assessed in all thymic lymphomas. The primer sets for the amplification of the entire *Ikaros* cDNA (exons 1–7) were *Ikaros* 1F and 7R(3) [15]. Sequencing to determine mutations in the splicing junction between exons 3 and 4, or exons 4 and 5 was performed using PCR fragments amplified from genomic DNA using LA Taq (Takara Shuzo Co., Shiga, Japan). The primer set for the junction between exons 3 and 4 was sense 3F(2), 5′-AGG CAT TCG ACT TCC TAA CG-3′ and antisense 4R, 5′-GGT TGC ACT GGA AAG GCC GT-3′. The primer set for the junction between exons 4 and 5 was sense 4F, 5′-GGT GAA CGG CCT TTC CAG TGC-3′ and antisense 5R, 5′-TGT TTA TAG CTC CGG CCA CAA T-3′. PCR products were purified using Quantum Prep Freeze N Squeeze DNA extraction spin columns (Bio-Rad, Hercules, CA), concentrated by ethanol precipitation and suspended in distilled water prior to sequencing. The primer set for the amplification of *p53* cDNA (between exons 5 and 9 containing the DNA-binding domain) was sense *p53* F(1), 5′-CCC TGT CAT CTT TTG TCC CTT-3′ and antisense *p53* R(1), 5′-CGC GGA TCT TGA GGG TGA AAT-3′. For the *ras* gene, the first, second and third exons of K*ras* were analyzed by single-strand conformation polymorphism (SSCP) analysis of genomic DNA followed by TA-cloning sequencing as described previously [27].

Sequencing was performed using the BigDye Terminator Cycle Sequencing FS Ready Reaction kit for both the direct and TA-cloning sequencing (PE Applied Biosystems, Foster City, CA) and the products were analyzed on an ABI PRISM 310 DNA Sequencer (PE Applied Biosystems). For direct sequencing, at a minimum, both forward and reverse sequences were determined for each sample. For TA-cloning, at least five clones from each sample were analyzed. Any mutations detected in cDNA were confirmed by analysis of the corresponding genomic DNA to exclude the possibility of false positives resulting from the errors during PCR amplification.

3. Results

3.1. Development of thymic lymphomas and phenotypic staging

Five-week-old mice were treated with ENU for 8 weeks. Thymic lymphomas developed in 75% (45/60) of the mice. The average latency period was 7 ± 4 weeks after the end of the treatment and the lifes-

pan of treated mice was 20 ± 4 weeks. These values are much shorter than those observed for lymphomas induced by X-irradiation (latency, 16 ± 3 weeks after treatment; lifespan, 22 ± 3 weeks) ($p < 0.01$) [14]. The mass of ENU-induced thymic lymphomas was 520 ± 34 mg compared with 486 ± 36 mg for X-ray-induced tumors (not significantly different; $p = 0.12$).

Expression of the surface antigens CD4, CD8, CD3, CD125 (IL2Rα), CD44, c-Kit, TCRαβ and TCRγδ was examined to classify the thymic lymphomas into stages of differentiation. Sixteen of the 19 thymic lymphomas (84%) were $CD4^+CD8^+$, 9 of which were immature $CD3^-$ with the remaining 7 being mature $CD3^+$. One thymic lymphoma was $CD4^+CD8^{\pm}CD3^+$, reflecting the mature differentiated stage of the $CD4^+$ single positive. The remaining two lymphomas were $CD4^{\pm}CD8^+CD3^-$ and $CD4^{\pm}CD8^-CD3^-$, both of which were at an immature stage. Expression of c-Kit and TCRγδ were negative in all the thymic lymphomas examined (data not shown). These results are consistent with the previous studies [21,28].

3.2. LOH status in chromosome 11

p53 and *Ikaros* are located on chromosome 11 in the telomeric (39.0 cM) and centromeric regions (6.0 cM), respectively. Ten microsatellite markers on chromosome 11 were used for allotyping in 27 thymic lymphomas. *p53* has been mapped close to *Acrb* and *Ikaros* has been mapped between *D11Mit62* and *D11Mit2* [14]. LOH was detected in 2/27 lymphomas (7%). These two tumors (S1603 and S1610) exhibited LOH at all loci examined, indicating non-disjunction as a mechanism of LOH. Thus, the frequency of LOH was low in ENU-induced thymic lymphomas compared with the LOH rates observed in radiation- (50%) or 1,3-butadiene-induced lymphomas (26%) [14,29].

3.3. Expression of Ikaros

We previously demonstrated that 25% of the radiation-induced thymic lymphomas from B6C3F1 mice have altered *Ikaros* expression (i.e., silencing or alternative splicing) [15]. The *Ikaros* expression pattern in ENU-induced lymphomas was essentially identical to that in the normal thymocytes (Fig. 1a), with concomitant expression of 750 and 490-bp products corresponding to *Ik1* and *Ik2*, respectively [30]. One

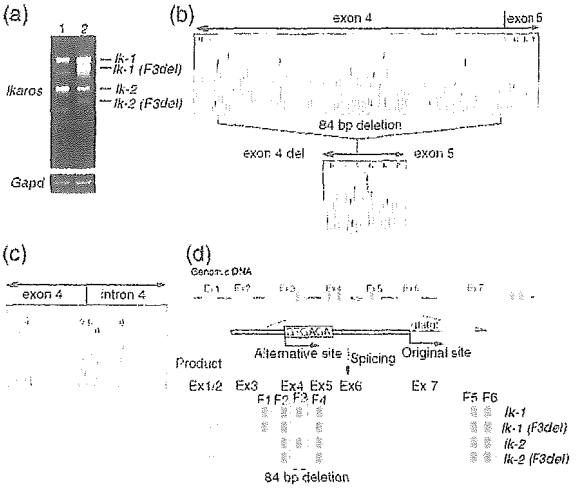

Fig. 1. Expression and sequence analysis of the shortened *Ikaros* isoform in ENU-induced thymic lymphoma S1624. (a) RT-PCR analysis of *Ikaros* expression in normal thymocytes from 6-week-old mice (lane 1) or in the thymic lymphoma S1624 (lane 2). Each cDNA sample was amplified with the primers for *Ikaros* (2F/7R) and *Gapd* (control). (b) Sequence analysis of *Ikaros* expressed in S1624. The upper panel depicts the sequence between exons 4 and 5 in *Ik1* or *Ik2* and the lower panel shows the sequence of the corresponding shortened fragment in S1624. Codons and amino acid sequences are shown above each sequence panel. An 84-bp deletion was found at the 3′ end of exon 4. (c) Heterozygous (t>t/g) point mutation in a splice donor site in intron 4 of S1624, as determined by direct sequencing. (d) Schematic presentation of genomic mutations and alternative splicing of *Ikaros* in S1624. A heterozygous mutation in intron 4 resulted in the creation of the mutant Ikaros isoforms *Ik-1 (F3del)* and *Ik-2 (F3del)* in addition to *Ik1* and *Ik2*.

lymphoma, S1624, expressed two additional isoforms of slightly reduced size relative to *Ik1* and *Ik2* (Fig. 1a). These results were confirmed by Western blotting (data not shown). Sequence analysis demonstrated that the shorter isoforms had an 84-bp deletion in the latter half of exon 4, resulting in the deletion of zinc-finger 3 within the N-terminal DNA-binding domain (Fig. 1b and d). We designated these internally deleted genes as *Ik1 (F3del)* and *Ik2 (F3del)*. No such *Ikaros* mutants have been reported previously. Cobb et al. [31] reported a deletion construct of *Ikaros dF3*, which is identical to *Ik (F3del)*, and showed loss of both DNA-binding activity and pericentromeric targeting ability in 3T3 fibroblasts.

We subsequently analyzed the genomic DNA sequence of the S1624 lymphoma between exons 4 and 5 of the *Ikaros* gene and identified a point mutation in

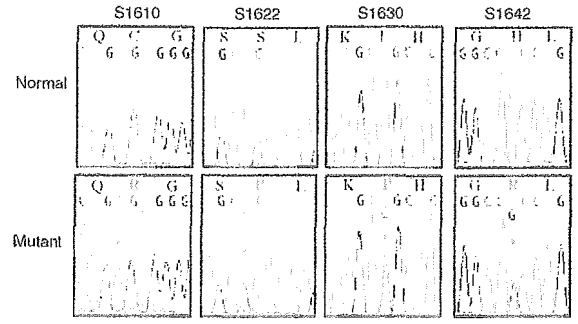

Fig. 2. Point mutations of *Ikaros* in ENU-induced thymic lymphomas. Each panel indicates codons and amino acid sequence for *Ikaros* (GenBank accession no. L03547 with insertion of exon 3) or mutants thereof. Arrows indicate the positions of base substitutions. The point mutation of S1610 (column 1) is homozygous while those of S1622 (column 2), S1630 (column 3) or S1642 (column 4) are heterozygous.

the splicing donor site within intron 4 (gtatgt > ggtatgt, Fig. 1c) that could potentially compromise donor function during pre-mRNA splicing. Consequently, the sequence GTGAGA in exon 4, located 84-bp upstream of the original splice donor site, was used as an altered (and novel) splice site. Because the point mutation was heterozygous, the wild-type allele underwent normal splicing as well. As a result, the S1624 lymphoma expressed the four alternative mRNAs *Ik1*, *Ik2*, *Ik1 (F3del)* and *Ik2 (F3del)* (Fig. 1d). This contrasts with the previous data in which no splice site mutations were found in the mouse thymic lymphomas and human leukemic cells expressing Ikaros isoforms *Ik4, Ik4 (del), Ik6, Ik8* and *Ik8 (del)* [9,15].

3.4. Point mutations of Ikaros

Point mutations of *Ikaros* have also been described in radiation- and 1,2-butadiene-induced thymic lymphomas [15,17,29]. Therefore, we examined *Ikaros* mutations in 26 ENU-induced thymic lymphomas. Sequence analysis of the entire *Ikaros* cDNA (exons 1–7) and the corresponding genomic DNA revealed point mutations in four thymic lymphomas (S1610, S1622, S1630, S1642; Fig. 2; Table 1). Three of them (S1622, S1630, S1643) were heterozygous at the mutation site. All four were the missense mutations in the N-terminal zinc finger DNA-binding domain. Three of the four mutations (S1610, S1630, S1642) were located in the C_2H_2 zinc-finger structure important for interaction with zinc and one (S1622) was located at a serine residue next to leucine, which is a conserved hydrophobic residue within an α-helix involved in zinc finger secondary structure. The distribution of the point mutations was distinct from that seen in radiation-induced lymphomas where mutations were more sparsely distributed and were accompanied by LOH [15]. All point mutations were T > C transitions.

3.5. Analysis of p53 mutations

Next, we analyzed thymic lymphoma samples for the mutations in *p53*. Eight tumors (S1594, S1607, S1610, S1633, S1634, S1641, S1642 and S1643) harbored missense mutations in the DNA-binding region (Table 1). Two tumors (S1607 and S1610) did not express p53 protein while the other six (S1594, S1633, S1634, S1641, S1642 and S1643) expressed high levels of p53 (data not shown). These results are consistent with a previous report that mutant p53 has an increased half-life and accumulates in the nucleus [32]. As was the case for *Ikaros*, the majority (88%, 7/8) of lymphomas with *p53* point mutations retained a wild-type *p53* allele except for S1610.

3.6. Point mutations of Kras

Frequent mutations of the K*ras* oncogene have been reported in nitroso compound-induced tumors [21,33]. Seven tumors (S1601, S1607, S1622, S1630, S1631, S1634 and S1644) had K*ras* gene mutations, five of which (S1607, S1622, S1630, S1631, and S1644) were in codon 12, one (S1634) in codon 59 and one (S1601) in codon 61. All K*ras* mutations were heterozygous and retained a wild-type allele. Two tumors (S1607 and S1622) harbored two mutations concomitantly, displaying two additional bands in SSCP analysis (Fig. 3a), that resulted in nine point mutations in total. Sequence analysis after TA-cloning of the K*ras* gene revealed that these lymphomas contained three types of sequence in codon 12, namely GGT (wild-type), GAT and TGT, at a ratio of 3:2:5 (Fig. 3b).

3.7. Mutation spectrum in ENU-induced thymic lymphomas

The mutation and LOH status for each ENU-induced thymic lymphoma is summarized in Table 1.

Table 1
Alteration of *p53*, *Ikaros* and *Kras* and LOH status of chromosome 11 in ENU-induced thymic lymphomas (TL)

Sample	Latency (days)	TL size (mg)	*Ikaros*				*P53*				*Kras*	
			Codon	Nucleotide (aa)	Location	LOH[a]	Codon	Nucleotide (aa)	Protein[b]	LOH[a]	Codon	Nucleotide (aa)
S1594	110	743				–	160	TAC > CAC (Y > H)	+	–		
S1601	117	ND[c]				–				–	61	CAA > CTA (Q > L)
S1607	121	345				–	210	CGC > TGC (R > C)	–	–	12	GGT > TGT (G > C)
												GGT > GAT (G > D)
S1610	122	431	150	TGT > CGT (C > R)	F2[d]	B	213	GTG > TTG (V > L)	–	B		
S1622	130	864	215	TCT > CCT (S > P)	F4[e]	–				–	12	GGT > TGT (G > C)
											12	GGT > GAT (G > D)
S1624	130	615	int4 + 2	gt > gg (del 169–196)	F3del[f]	–				–		
S1630	132	994	166	CTG > CCG (L > P)	F2[d]	–				–	12	GGT > TGT (G > C)
S1631	136	309				–				–	12	GGT > GAT (G > D)
S1633	136	595				–	213	GTG > ATG (V > M)	+	–		
S1634	139	577				–	243	ATG > AAG (M > K)	+	–	59	GCA > GAA (A > E)
S1641	143	818				–	243	ATG > AAG (M > K)	+	–		
S1642	145	711	191	CAC > CGC (H > R)	F3[d]	–	190	CAT > CTT (H > L)	+	–		
S1643	145	892				–	194	GTG > GAG (V > E)	+	–		
S1644	145	877				–				–	12	GGT > GAT (G > D)

[a] Lost allele: B, B6; (–), heterozygous.
[b] Expression status of p53 protein: (+), over-expression; (–), no expression (normal type).
[c] ND: not determined.
[d] Mutation was located in the C_2H_2 zinc-finger structure for interaction with zinc.
[e] Mutation was located in an α-helix structure in the zinc-finger protein.
[f] Described in Fig. 1.

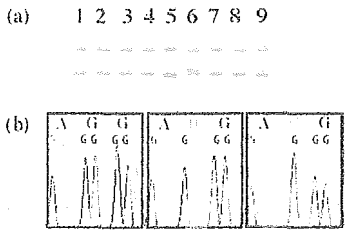

Fig. 3. Detection of K*ras* mutations in ENU-induced thymic lymphomas. (a) PCR-SSCP analysis. Lane 1 shows the *Kras* pattern from normal thymocytes, and lanes 2, 3, 4, 7 and 8 represent thymocytes from thymic lymphomas without K*ras* mutations. Lanes 5 (S1631), 6 (S1630) and 9 (S1607) show altered patterns. (b) Sequence analysis after TA-cloning of S1607 (lane 9 in panel a). Three types of sequence, GGT, GAT and TGT, were found at codon 12 (panel b).

In *Ikaros*, four of the five mutations (80%) were T > C. In *p53*, four of the eight mutations (50%) were T > A and two were G > A (25%). In K*ras*, four of the nine mutations were G > A (44%) and another four were G > T (44%). These results are in good agreement with the evidence that ENU produces significant levels of alkylation at oxygen atoms such as the O^6 position of guanine and the O^4 position of thymine in DNA [18]. The results also indicate, however, that the spectrum of base substitutions is different among these genes.

It is also noteworthy that 43% (6/14) of the lymphomas harbored double mutations. S1610 and S1642 harbored mutations in both *Ikaros* and *p53*. S1607 and S1634 had mutations in *p53* and K*ras*. S1622 and S1630 had mutations in *Ikaros* and K*ras*. In all, 14 of the 27 lymphomas (52%) had mutations in at least one of the three genes examined and most of these lymphomas also retained a wild-type allele of the *p53*, *Ikaros* and K*ras* genes.

4. Discussion

This study revealed point mutations in the tumor suppressor genes *p53* and *Ikaros* in 8 (30%) and 5 (19%) of the 27 ENU-induced thymic lymphomas, respectively. This was often accompanied by the retention of a wild-type allele (in 7/8 [88%] of *p53* mutations and 4/5 [80%] of *Ikaros* mutations). One of the *Ikaros* mutations was located at the splice donor site, generating a novel splice isoform lacking zinc finger 3, *Ik (F3del)*. Together with 7 lymphomas with K*ras* oncogene mutations (23%), 14 of the 27 (52%) thymic lymphomas harbored point mutations in at least 1 of the 3 genes examined.

Tumor suppressor genes can be inactivated by point mutations or deletions according to Knudson's "two-hit" hypothesis [1]. However, some tumor suppressor genes with particular types of mutations act as oncogenes in a dominant manner, probably by forming oligomeric complexes with wild-type or other proteins that results in the loss of wild-type protein function [5,34]. Recently, mice were produced having targeted point mutations of *p53* [35,36]. Mice heterozygous for a mutation in codon 172, R172H differed from p53+/− mice in tumor spectrum and metastatic frequency. Interestingly, loss of a wild-type *p53* allele was rarely observed in the tumors [35]. Cells from two other mice heterozygous for *p53* point mutations, R270H and P275S, exhibited delayed transcriptional activation of *p53* downstream target genes upon exposure to gamma-rays. They also showed severe defects in p53-dependent apoptosis, supporting negative dominance over wild-type p53 [36].

A *Plastic* mouse strain was recently developed that has the same point mutation as *Ikaros*, H191R, found in lymphoma S1642 (Fig. 2). It has been demonstrated that mice heterozygous for H191R, $Ikaros^{Plastic/+}$, develop leukemia/lymphomas frequently within 4 months after birth [37]. Although the lymphomas developed in $Ikaros^{Plastic/+}$ have not been examined for the loss of wild-type alleles, the S1642 lymphoma in the present study showed retention of a wild-type *Ikaros* allele. These data suggest negative dominance of this *Ikaros* point mutation in vivo. However, functional studies are required to confirm that this is indeed the case. There are other reports of tumor suppressor genes that are exceptions to the classical version of Knudson's two-hit theory [38,39]. These include *Caveolin-1* and *Smad4*. A point mutation, P132L, in codon 132 of *Caveolin-1* has been reported in 16% of the primary human breast cancers but no loss of heterozygosity of the wild-type *Caveolin-1* gene was observed [40]. A point mutation in *Smad4* has been frequently observed in pancreatic and colon cancers. Expression of Smad4 carrying an R497H mutation antagonized TGF-β signaling in a dominant-negative manner [41], consistent with the clinical observations that only one *Smad4* allele is affected in some cancers [42]. It seems likely that the cancers harboring heterozygous point mutations of Caveolin-1 and Smad4 are inactive for wild-type cave-

olin and Smad4 function because both Caveolin-1 and Smad4 form homo- and heteromeric complexes, respectively.

One cannot exclude the possibility, however, that inactivating one *p53* allele through the mutation results in a cellular phenotype caused by gene dosage reduction, a phenomenon previously described by others in p53+/− knockout mice [43]. Indeed, LOH at both *p53* and *Ikaros* loci without an additional point mutation in the other allele was found in lymphoma S1603. In addition, the p53 mutations found in the ENU-induced lymphomas are not the well known hot-spot mutations frequently found in the other tumor types that were previously shown to display dominant-negative activity [36,44]. These lines of evidence indicate that carcinogenesis occurs despite the production of wild-type tumor suppressor proteins in contrast to the standard definition of tumor suppressor genes.

In addition to the point mutations, alternative use of transcriptional initiation sites or alternative splicing that results in a lack of DNA-binding or transactivation activity may be another mechanism(s) to generate dominant-negative tumor suppressor proteins. N-terminally truncated p73 and several Ikaros isoforms (Ik4, Ik6 and Ik8) lacking DNA-binding domains have been reported in some tumors [12,45]. We previously reported that lymphomas expressing Ikaros splice variants (Ik4, Ik6 and Ik8) retain a wild-type *Ikaros* allele [15]. In the present study, lymphoma S1624 expressed a novel Ik (F3del) isoform caused by a point mutation at the splice site but retained a wild-type allele.

Knudson's two-hit model of tumor suppressor genes supposes biallelic disruption which frequently involves loss of a wild-type allele via deletion and/or mitotic recombination. LOH has previously been useful for predicting tumor suppressor loci. However, a growing number of reports have described candidate tumor suppressors that do not conform to this standard definition. These include loci that exhibit negative dominancy and haploinsufficiency. Indeed, we demonstrated here that lymphomas induced by ENU, which is effective at inducing point mutations but not in deletion and/or recombination events, frequently harbored mutations of tumor suppressor genes such as *p53* and *Ikaros* without accompanying LOH. Therefore, to obtain a more complete picture of carcinogenesis, it will be important to examine mutations/alterations of other tumor suppressor genes whose loci do not demonstrate LOH.

In summary, our data suggest that ENU facilitates T cell lymphomagenesis by dominant-negative inactivation of tumor suppressor gene function as well as by oncogene (*ras*) activation.

Acknowledgments

We thank Ms. E. Obara, Ms. M. Takada and Ms. K. Yajima for technical assistance, and the Division of Animal Facility staff for help with the laboratory analysis and maintenance of animals. We also thank Dr. T. Ogiu for his encouragement throughout the course of our research. This study was supported partly through a grant of "Ground-based Research Announcement for Space Utilization" promoted by the Japan Space Forum, and a grant of Long-rang Research Initiative (LRI) by Japan Chemical Industry Association (JCIA).

References

[1] A.G. Knudson Jr., Mutation and cancer: statistical study of retinoblastoma, Proc. Natl. Acad. Sci. U.S.A. 68 (1971) 820–823.
[2] A.G. Knudson, Antioncogenes and human cancer, Proc. Natl. Acad. Sci. U.S.A. 90 (1993) 10914–10921.
[3] J.M. Nigro, S.J. Baker, A.C. Preisinger, J.M. Jessup, R. Hostetter, K. Cleary, S.H. Bigner, N. Davidson, S. Baylin, P. Devilee, et al., Mutations in the *p53* gene occur in diverse human tumour types, Nature 342 (1989) 705–708.
[4] R. Mazars, L. Spinardi, M. BenCheikh, J. Simony-Lafontaine, P. Jeanteur, C. Theillet, p53 mutations occur in aggressive breast cancer, Cancer Res. 52 (1992) 3918–3923.
[5] P. Wang, M. Reed, Y. Wang, G. Mayr, J.E. Stenger, M.E. Anderson, J.F. Schwedes, P. Tegtmeyer, p53 domains: structure, oligomerization, and transformation, Mol. Cell. Biol. 14 (1994) 5182–5191.
[6] K.G. McLure, P.W. Lee, How p53 binds DNA as a tetramer, EMBO J. 17 (1998) 3342–3350.
[7] L. Sun, N. Heerema, L. Crotty, X. Wu, C. Navara, A. Vassilev, M. Sensel, G.H. Reaman, F.M. Uckun, Expression of dominant-negative and mutant isoforms of the antileukemic transcription factor Ikaros in infant acute lymphoblastic leukemia, Proc. Natl. Acad. Sci. U.S.A. 96 (1999) 680–685.
[8] L. Sun, M.L. Crotty, M. Sensel, H. Sather, C. Navara, J. Nachman, P.G. Steinherz, P.S. Gaynon, N. Seibel, C. Mao, A. Vassilev, G.H. Reaman, F.M. Uckun, Expression of dominant-negative Ikaros isoforms in T-cell acute lymphoblastic leukemia, Clin. Cancer Res. 5 (1999) 2112–2120.
[9] L. Sun, P.A. Goodman, C.M. Wood, M.L. Crotty, M. Sensel, H. Sather, C. Navara, J. Nachman, P.G. Steinherz, P.S. Gaynon, N. Seibel, A. Vassilev, B.D. Juran, G.H. Reaman, F.M. Uckun,

Expression of aberrantly spliced oncogenic Ikaros isoforms in childhood acute lymphoblastic leukemia, J. Clin. Oncol. 17 (1999) 3753–3766, see comments.

[10] H. Nakayama, F. Ishimaru, N. Avitahl, N. Sezaki, N. Fujii, K. Nakase, Y. Ninomiya, A. Harashima, J. Minowada, J. Tsuchiyama, K. Imajoh, T. Tsubota, S. Fukuda, T. Sezaki, K. Kojima, M. Hara, H. Takimoto, S. Yorimitsu, I. Takahashi, A. Miyata, S. Taniguchi, Y. Tokunaga, H. Gondo, Y. Niho, M. Harada, et al., Decreases in Ikaros activity correlate with blast crisis in patients with chronic myelogenous leukemia, Cancer Res. 59 (1999) 3931–3934.

[11] S. Winandy, P. Wu, K. Georgopoulos, A dominant mutation in the *Ikaros* gene leads to rapid development of leukemia and lymphoma, Cell 83 (1995) 289–299.

[12] L. Sun, A. Liu, K. Georgopoulos, Zinc finger-mediated protein interactions modulate Ikaros activity, a molecular control of lymphocyte development, EMBO J. 15 (1996) 5358–5369.

[13] B. Morgan, L. Sun, N. Avitahl, K. Andrikopoulos, T. Ikeda, E. Gonzales, P. Wu, S. Neben, K. Georgopoulos, Aiolos, a lymphoid restricted transcription factor that interacts with Ikaros to regulate lymphocyte differentiation, EMBO J. 16 (1997) 2004–2013.

[14] Y. Shimada, M. Nishimura, S. Kakinuma, M. Okumoto, T. Shiroishi, K.H. Clifton, S. Wakana, Radiation-associated loss of heterozygosity at the Znfn1a1 (Ikaros) locus on chromosome 11 in murine thymic lymphomas, Radiat. Res. 154 (2000) 293–300.

[15] S. Kakinuma, M. Nishimura, S. Sasanuma, K. Mita, G. Suzuki, Y. Katsura, T. Sado, Y. Shimada, Spectrum of Znfn1a1 (Ikaros) inactivation and its association with loss of heterozygosity in radiogenic T-cell lymphomas in susceptible B6C3F1 mice, Radiat. Res. 157 (2002) 331–340.

[16] P. Lopez-Nieva, J. Santos, J. Fernandez-Piqueras, Defective expression of Notch1 and Notch2 in connection to alterations of c-Myc and Ikaros in gamma-radiation-induced mouse thymic lymphomas, Carcinogenesis 25 (2004) 1299–1304.

[17] H. Okano, Y. Saito, T. Miyazawa, T. Shinbo, D. Chou, S. Kosugi, Y. Takahashi, S. Odani, O. Niwa, R. Kominami, Homozygous deletions and point mutations of the *Ikaros* gene in gamma-ray-induced mouse thymic lymphomas, Oncogene 18 (1999) 6677–6683.

[18] T. Shibuya, K. Morimoto, A review of the genotoxicity of 1-ethyl-1-nitrosourea, Mutat. Res. 297 (1993) 3–38.

[19] M.C. Poirier, R.M. Santella, A. Weston, Carcinogen macromolecular adducts and their measurement, Carcinogenesis 21 (2000) 353–359.

[20] E.W. Newcomb, J.J. Steinberg, A. Pellicer, *ras* oncogenes and phenotypic staging in *N*-methylnitrosourea- and gamma-irradiation-induced thymic lymphomas in C57BL/6J mice, Cancer Res. 48 (1988) 5514–5521.

[21] Y. Shimada, M. Nishimura, S. Kakinuma, T. Ogiu, H. Fujimoto, A. Kubo, J. Nagai, K. Kobayash, K. Tano, S. Yoshinaga, K.K. Bhakat, Genetic susceptibility to thymic lymphomas and K-*ras* gene mutation in mice after exposure to X-rays and *N*-ethyl-*N*-nitrosourea, Int. J. Radiat. Biol. 79 (2003) 423–430.

[22] E. Romach, J. Moore, S. Rummel, E. Richie, Influence of sex and carcinogen treatment protocol on tumor latency and frequency of K-*ras* mutations in *N*-methyl-*N*-nitrosourea-induced lymphomas, Carcinogenesis 15 (1994) 2275–2280.

[23] I.P. Perez de Castro, M. Malumbres, J. Santos, A. Pellicer, J. Fernandez-Piqueras, Cooperative alterations of Rb pathway regulators in mouse primary T cell lymphomas, Carcinogenesis 20 (1999) 1675–1682.

[24] S.W. Wijnhoven, P.P. Van Sloun, H.J. Kool, G. Weeda, R. Slater, P.H. Lohman, A.A. van Zeeland, H. Vrieling, Carcinogen-induced loss of heterozygosity at the Aprt locus in somatic cells of the mouse, Proc. Natl. Acad. Sci. U.S.A. 95 (1998) 13759–13764.

[25] S.W. Wijnhoven, H.J. Kool, C.M. van Teijlingen, A.A. van Zeeland, H. Vrieling, Loss of heterozygosity in somatic cells of the mouse. An important step in cancer initiation, Mutat. Res. 473 (2001) 23–36.

[26] M. Nishimura, S. Kakinuma, S. Wakana, A. Mukaigawara, K. Mita, T. Sado, T. Ogiu, Y. Shimada, Reduced sensitivity to and ras mutation spectrum of *N*-ethyl-*N*-nitrosourea-induced thymic lymphomas in adult C.B-17 scid mice, Mutat. Res. 486 (2001) 275–283.

[27] M. Nishimura, S. Wakana, S. Kakinuma, K. Mita, H. Ishii, S. Kobayashi, T. Ogiu, T. Sado, Y. Shimada, Low frequency of *Ras* gene mutation in spontaneous and gamma-ray-induced thymic lymphomas of scid mice, Radiat. Res. 151 (1999) 142–149.

[28] Y. Shimada, M. Nishimura, S. Kakinuma, T. Takeuchi, T. Ogiu, G. Suzuki, Y. Nakata, S. Sasanuma, K. Mita, T. Sado, Characteristic association between K-*ras* gene mutation with loss of heterozygosity in X-ray-induced thymic lymphomas of the B6C3F1 mouse, Int. J. Radiat. Biol. 77 (2001) 465–473.

[29] A. Karlsson, P. Soderkvist, S.M. Zhuang, Point mutations and deletions in the znfn1a1/*Ikaros* gene in chemically induced murine lymphomas, Cancer Res. 62 (2002) 2650–2653.

[30] K. Georgopoulos, Transcription factors required for lymphoid lineage commitment, Curr. Opin. Immunol. 9 (1997) 222–227.

[31] B.S. Cobb, S. Morales-Alcelay, G. Kleiger, K.E. Brown, A.G. Fisher, S.T. Smale, Targeting of Ikaros to pericentromeric heterochromatin by direct DNA binding, Genes Dev. 14 (2000) 2146–2160.

[32] A.M. Davidoff, P.A. Humphrey, J.D. Iglehart, J.R. Marks, Genetic basis for p53 overexpression in human breast cancer, Proc. Natl. Acad. Sci. U.S.A. 88 (1991) 5006–5010.

[33] O. Brathwaite, W. Bayona, E.W. Newcomb, p53 mutations in C57BL/6J murine thymic lymphomas induced by gamma-irradiation and *N*-methylnitrosourea, Cancer Res. 52 (1992) 3791–3795.

[34] A. Willis, E.J. Jung, T. Wakefield, X. Chen, Mutant p53 exerts a dominant negative effect by preventing wild-type p53 from binding to the promoter of its target genes, Oncogene 23 (2004) 2330–2338.

[35] G. Liu, T.J. McDonnell, R. Montes de Oca Luna, M. Kapoor, B. Mims, A.K. El-Naggar, G. Lozano, High metastatic potential in mice inheriting a targeted p53 missense mutation, Proc. Natl. Acad. Sci. U.S.A. 97 (2000) 4174–4179.

[36] A. de Vries, E.R. Flores, B. Miranda, H.M. Hsieh, C.T. van Oostrom, J. Sage, T. Jacks, Targeted point mutations of p53 lead to dominant-negative inhibition of wild-type p53 function, Proc. Natl. Acad. Sci. U.S.A. 99 (2002) 2948–2953.

[37] P. Papathanasiou, A.C. Perkins, B.S. Cobb, R. Ferrini, R. Sridharan, G.F. Hoyne, K.A. Nelms, S.T. Smale, C.C. Goodnow, Widespread failure of hematolymphoid differentiation caused by a recessive niche-filling allele of the Ikaros transcription factor, Immunity 19 (2003) 131–144.

[38] A.J. Paige, Redefining tumour suppressor genes: exceptions to the two-hit hypothesis, Cell Mol. Life Sci. 60 (2003) 2147–2163.

[39] P. Hohenstein, Tumour suppressor genes-one hit can be enough, PLoS Biol. 2 (2004) 40.

[40] H. Lee, D.S. Park, B. Razani, R.G. Russell, R.G. Pestell, M.P. Lisanti, Caveolin-1 mutations (P132L and null) and the pathogenesis of breast cancer: caveolin-1 (P132L) behaves in a dominant-negative manner and caveolin-1 (–/–) null mice show mammary epithelial cell hyperplasia, Am. J. Pathol. 161 (2002) 1357–1369.

[41] C. Kuang, Y. Chen, Tumor-derived C-terminal mutations of Smad4 with decreased DNA binding activity and enhanced intramolecular interaction, Oncogene 23 (2004) 1021–1029.

[42] M. Miyaki, T. Iijima, M. Konishi, K. Sakai, A. Ishii, M. Yasuno, T. Hishima, M. Koike, N. Shitara, T. Iwama, J. Utsunomiya, T. Kuroki, T. Mori, Higher frequency of *Smad4* gene mutation in human colorectal cancer with distant metastasis, Oncogene 18 (1999) 3098–3103.

[43] S. Venkatachalam, Y.P. Shi, S.N. Jones, H. Vogel, A. Bradley, D. Pinkel, L.A. Donehower, Retention of wild-type p53 in tumors from p53 heterozygous mice: reduction of p53 dosage can promote cancer formation, EMBO J. 17 (1998) 4657–4667.

[44] M.G. van Oijen, P.J. Slootweg, Gain-of-function mutations in the tumor suppressor gene *p53*, Clin. Cancer Res. 6 (2000) 2138–2145.

[45] A.I. Zaika, N. Slade, S.H. Erster, C. Sansome, T.W. Joseph, M. Pearl, E. Chalas, U.M. Moll, DeltaNp73, a dominant-negative inhibitor of wild-type p53 and TAp73, is up-regulated in human tumors, J. Exp. Med. 196 (2002) 765–780.

Enhancement of Cisplatin-Induced Apoptosis and Caspase 3 Activation by Depletion of Mitochondrial DNA in a Human Osteosarcoma Cell Line

HSIU-CHUAN YEN,[a] YI-CHIA TANG,[a] FAN-YI CHEN,[a] SHIH-WEI CHEN,[a] AND HIDEYUKI J. MAJIMA[b]

[a]*Graduate Institute of Medical Biotechnology and School of Medical Technology, Chang Gung University, Tao-Yuan, Taiwan*

[b]*Department of Oncology, Kagoshima University Graduate School of Medical and Dental Sciences, Kagoshima, Japan*

ABSTRACT: **Cisplatin is an anticancer drug that can induce apoptosis. In this study, we investigated the effect of mitochondrial DNA (mtDNA) depletion on cisplatin-induced cell death using a human osteosarcoma cell line (143B) and mtDNA-depleted 143B cells (143B-ρ^0). Results showed that cisplatin decreased cell survival in 143B-ρ^0 cells. Moreover, cisplatin induced a greater extent of apoptosis-associated DNA fragmentation and caspase 3 activation in 143B-ρ^0 cells. The release of mitochondrial cytochrome *c* into cytosol by cisplatin was enhanced more obviously in 143B cells than in 143B-ρ^0 cells; however, in the control group of 143B-ρ^0 cells, it was already dramatically greater. Depletion of mtDNA may increase sensitivity of cells to cisplatin-induced apoptosis by enhancing caspase 3 activation via both cytochrome *c*–dependent and –independent pathways.**

KEYWORDS: **cisplatin; mitochondrial DNA; apoptosis; caspase 3; cytochrome *c***

INTRODUCTION

Cisplatin (cis-diamminedichloroplatinum [II]; CDDP) is a chemotherapeutic agent that is known to inhibit DNA replication by cross-linking DNA.[1] It has been shown that reactive oxygen species could be important in CDDP-induced apoptosis.[2] It has also been indicated that suppression of apoptosis was important in CDDP resistance in cancer cells,[3] and DNA platination or p53 status did not necessarily determine the sensitivity of cancer cells to CDDP-induced apoptosis.[4] In the mechanisms leading to apoptosis, activation of caspase 3 can result from different upstream caspases or release of the Smac/DIABLO protein from mitochondria independent of other caspases.[5] It has been indicated that CDDP induced apoptosis via release of mitochondrial cytochrome *c* into cytosol with subsequent activation of

Address for correspondence: Hsiu-Chuan Yen, Ph.D., Graduate Institute of Medical Biotechnology, Chang Gung University, 259 Wen-Hwa 1st Rd., Kwei-Shan, Tao-Yuan 333, Taiwan. Voice: +886-3-2118800 ext. 5207; fax: +886-3-2118692.
yen@mail.cgu.edu.tw

Ann. N.Y. Acad. Sci. 1042: 516–522 (2005).
doi: 10.1196/annals.1338.047

caspase 9 and then caspase 3.[3] However, activation of caspase 8 upstream of caspase 3 has also been demonstrated.[6]

Human mitochondrial DNA (mtDNA) is a circular DNA with 16,569 bp that encodes 13 subunits of complexes I, III, IV, and V of oxidative phosphorylation.[7] Although it has been shown that CDDP can cause mtDNA damage,[8] the role of mtDNA in CDDP-induced apoptosis is not clear. In this study, we compared cell survival, extent of apoptosis, activation of caspase 3, and cytochrome *c* release in 143B and 143B-ρ^0 cells following CDDP treatment.

MATERIALS AND METHODS

The human osteosarcoma cell line, 143B cells (thymidine kinase deficient, TK), and 143B-ρ^0 cells (clone 143B-87) lacking mtDNA were obtained from Dr. Douglas Wallace at the University California, Irvine, CA.[9,10] The absence of mitochondrial gene expression has also been previously confirmed.[11] Both cell lines were cultured in high-glucose (4.5 g/L) Dulbecco's modified Eagle's medium supplemented with 10% fetal bovine serum, 110 μg/mL pyruvate, and 50 μg/mL uridine.

Evaluation of Cell Survival following CDDP Treatment

The colony formation assay was used to test the clonogenic ability of cells. Approximately 200 cells were plated on 60-mm dishes for 24 h and exposed to various doses of CDDP for another 24 h.The number of visible colonies grown from single cells was counted after staining cells with crystal violet to evaluate cell survival following CDDP treatment.[12] The threshold to define a colony was set at 50 cells per colony, which was much less than the number of cells in regular colonies of control dishes.

Detection of Apoptosis-Associated Nucleosomal Ladder

Total genomic DNA was isolated from cells using the Puregene DNA Isolation Kits from Gentra Systems (Minneapolis, MN). The ApoAlert ligation-mediated (LM)–PCR Ladder Assay kit from BD Biosciences Clontech (Palo Alto, CA) was used to determine the presence of nucleosomal ladder. The PCR products were electrophoresed in a 1.5% agarose gel containing ethidium bromide.

Measurement of Caspase 3 Activity

The ApoAlert Caspase Fluorescent Assay kit from BD Biosciences Clontech was used. A total of 10^6 cells were harvested, and supernatant from lysed cells was incubated with the substrate, DEVD-AFC (7-amino-4-trifluoromethyl coumarin), for 1 h at 37°C. Cleavage of the substrate by active caspase 3 resulted in the increase of fluorescence (excitation = 400 nm and emission = 505 nm), which was recorded by a 96-well fluorometer. The reading from no-substrate control was subtracted.

Western Blot Analysis for Detecting Cytochrome c *Release*

Cells were homogenized in mitochondrial isolation solution (0.225 M mannitol, 0.075 M sucrose, 1 mM EGTA, pH 7.4) containing the protease inhibitor cocktail

from Roche (Mannheim, Germany) and centrifuged at 600 × *g*. The supernatant was centrifuged at 10,000 × *g*, and the final supernatant was the cytosolic fraction without nuclear and mitochondrial fractions. The final pellet was washed and resuspended in 50 mM potassium phosphate buffer (pH 7.4) containing 0.5% Triton X-100 and saved as the mitochondrial fraction. Proteins were size-separated by SDS–polyacrylamide gel electrophoresis and analyzed for cytochrome *c*, actin, and Mn superoxide dismutase (MnSOD) using antibodies obtained from BD Pharmingen (San Diego, CA), Chemicon (Temecula, CA), and Upstate (Charlottesville, VA), respectively.

Statistical Analysis

Analysis of variance (ANOVA) was used to compare the difference among multiple groups using SASfor Windows version 8.1 (SAS Institute, Cary, NC). Data are presented as mean ± standard deviation.

RESULTS AND DISCUSSION

Results of cell survival assay are shown in FIGURE 1. The doses of drug that inhibited 50% and 90% of colony formation, IC_{50} and IC_{90}, were calculated from three independent experiments.[12] The IC_{50} for 143B and 143B-ρ^0 cells was 0.37 ± 0.01 and 0.24 ± 0.01 μg/mL, respectively; and the IC_{90} for 143B cells and 143B-ρ^0 cells was 0.77 ± 0.12 and 0.42 ± 0.03 μg/mL, respectively. Those results indicated that CDDP resulted in much lower cell survival in 143B-ρ^0 than in 143B cells, which could be caused by enhanced apoptosis or necrosis.

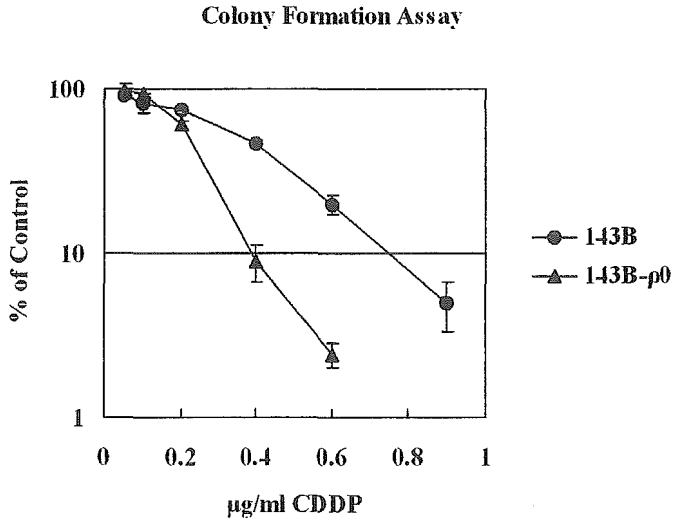

FIGURE 1. Cell survival curve following CDDP treatment obtained from colony formation assay. There are three dishes per group. The y-axis is in log scale.

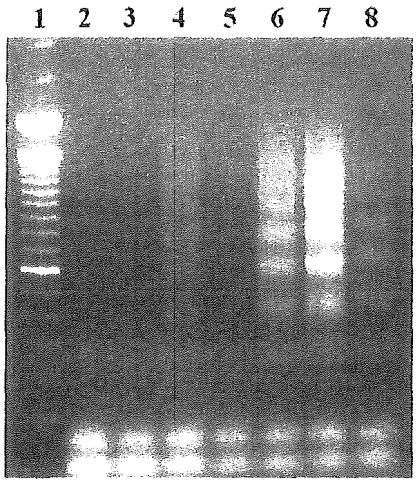

FIGURE 2. Detection of nucleosomal DNA ladder by LM-PCR. Lanes 1, 100-bp ladder; 2, 134B-control; 3, 143B-0.5 μg/mL CDDP; 4, 143B-1 μg/mL CDDP; 5, ρ^0-control; 6, ρ^0-0.5 μg/mL; 7, ρ^0-1 μg/mL; 8, positive control (calf thymus DNA).

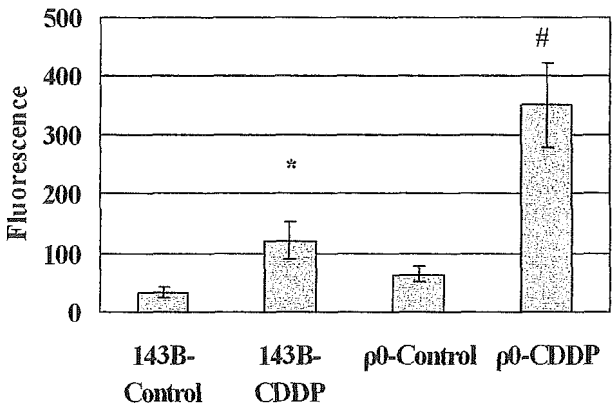

FIGURE 3. Caspase 3 activities following 24-h CDDP treatment (0.5 μg/mL). $^*P = .01$ for 143B-control versus 143B-CDDP; $^\#P < 0.0001$ for ρ^0-control versus ρ^0-CDDP. There are four replicates for each group.

We next investigated the effect of CDDP on apoptosis in these two cell lines. Results of LM-PCR (FIG. 2) demonstrated that 24-h CDDP treatment (0.5 and 1 μg/mL) induced a greater extent of apoptosis-associated DNA fragmentation in 143B-ρ^0 cells. Moreover, FIGURE 3 shows that 24-h CDDP treatment (0.5 μg/mL) increased caspase 3 activities in both cells. Two-way ANOVA revealed that the increase in 143B-ρ^0 cells was greater ($P = 0.0003$). Therefore, enhancement of CDDP-induced cell death by depletion of mtDNA was correlated with the increase in DNA fragmentation and caspase 3 activation.

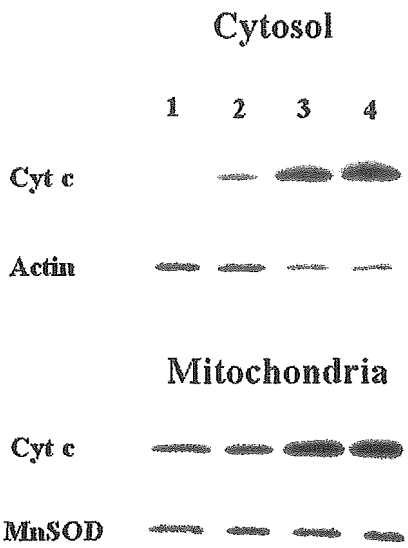

FIGURE 4. Western blot analysis for detection of cytochrome c release. Lanes 1, 2, 3, and 4 represent 143B-control, 143B-CDDP, ρ^0-control, and ρ^0-CDDP, respectively.

Furthermore, results of Western blot analysis (FIG. 4) showed that the amount of cytochrome c released into cytosol, relative to that of actin, was markedly increased by 24-h CDDP treatment (0.5 μg/mL) in 143B cells. The level of cytochrome *c* in cytosol was significantly higher in the control of 143B-ρ^0 cells than in 143B cells, although the increase after CDDP treatment was less obvious in 143B-ρ^0 cells. That could be due to the status of mitochondrial injury or a compensatory increase in cytochrome *c* expression because its level in mitochondria was also augmented in 143B-ρ^0 cells compared with that of MnSOD (FIG. 4). However, this increase did not lead to a proportional increase in the basal caspase 3 activity (FIG. 3), suggesting that 143B-ρ^0 cells could have become less sensitive to the death signal of cytochrome *c*, such as by suppression of apoptosome formation and caspase 9 activation,[5] during the stage without apoptotic insult. Persistent presence of higher levels of cytosolic cytochrome *c* in 143B-ρ^0 cells could result in greater caspase 3 activation by CDDP (FIG. 3), although cytochrome *c*–independent pathways might be also involved.

It has been shown that apoptosis and cytochrome *c* release induced by staurosporine were not altered following mtDNA depletion, demonstrating that those pathways were not impaired in ρ^0 cells.[10,13] However, apoptosis and translocation of cytochrome *c* were suppressed in ρ^0 cells after the treatment of tumor necrosis factor-related apoptosis–induced ligand (TRAIL),[14] whereas mtDNA depletion enhanced CDDP-induced apoptosis as shown by this study. Therefore, the use of ρ^0 cells has revealed diverse roles of mtDNA in apoptosis depending on the apoptotic stimuli used. Liang and Ullyatt also showed that CDDP-induced apoptosis was increased in ρ^0 cells derived from a lymphoma cell line (U937 cells) that was assessed by morphological changes, but they did not investigate any related apoptotic pathways.[15]

Our results first indicate that enhanced caspase 3 activation plays an important role in increased CDDP-induced cell death in 143B-ρ^0 cells. A higher degree of cytochrome *c* release in 143B-ρ^0 cells before treatment may be an important role, but mechanisms independent of cytochrome *c* release could be also enhanced, such as augmented activation of caspase 8 and release of Smac/DIABLO protein from mitochondria. Other mechanisms related to cytochrome *c*, such as the formation of apoptosome with apoptotic protease activating factor 1 (Apaf-1) and nitrosylation of cytochrome *c*, could be also important.[5,16] On the other hand, the existence of caspase-independent pathways in CDDP-induced apoptosis has been indicated.[17] Therefore, the role of caspase-independent mechanisms, such as release of apoptosis-inducing factor (AIF) from mitochondria, remains to be elucidated.[5] Furthermore, because mitochondrial dysfunction is known to induce oxidative stress and alter expression of nuclear genes,[7] chronic perturbation of redox status may result in different signaling pathways of cell death in response to CDDP in ρ^0 cells because CDDP can also increase oxidative stress.[1,2] However, as shown by this study, it is clear that the caspase-dependent pathway is, at least, a mechanism leading to increased extent of apoptosis by CDDP following mtDNA depletion in 143B cells.

ACKNOWLEDGMENTS

This work is supported by Grant CMRP1230 from Chang Gung Memorial Hospital, Taiwan.

REFERENCES

1. SIDDK, Z.H. 2003. Cisplatin: mode of cytotoxic action and molecular basis of resistance. Oncogene **22:** 7265–7279.
2. BAEK, S.M., C.H. KWON, J.H. KIM, *et al.* 2003. Differential roles of hydrogen peroxide and hydroxyl radical in cisplatin-induced cell death in renal proximal tubular epithelial cells. J. Lab. Clin. Med. **142:** 178–186.
3. MUELLER, T., W. VOIGT, H. SIMON, *et al.* 2003. Failure of activation of caspase-9 induces a higher threshold for apoptosis and cisplatin resistance in testicular cancer. Cancer Res. **63:** 513–522.
4. BURGER, H., K. NOOTER, A.W. BOERSMA, *et al.* 1997. Lack of correlation between cisplatin-induced apoptosis, p53 status and expression of Bcl-2 family proteins in testicular germ cell tumor cell lines. Int. J. Cancer **73:** 592–599.
5. HENGARTNER, M.O. 2000. The biochemistry of apoptosis. Nature **407:** 770–776.
6. HOTTA, T., H. SUZUKI, S. NAGAI, *et al.* 2003. Chemotherapeutic agents sensitize sarcoma cell lines to tumor necrosis factor-related apoptosis-inducing ligand-induced casepase-8 activation, apoptosis and loss of mitochondrial membrane potential. J. Orthop. Res. **21:** 949–957.
7. WALLACE, D.C. 1999. Mitochondrial diseases in man and mouse. Science **283:** 1482–1488.
8. OLIVERO, O.A., P.K. CHANG, D.M. LOPEZ-LARRAZA, *et al.* 1997. Preferential formation and decreased removal of cisplatin-DNA adducts in Chinese hamster ovary cell mitochondrial DNA as compared to nuclear DNA. Mutat. Res. **391:** 79–86.
9. TROUNCE, I., S. NEILL & D.C. WALLACE. 1994. Cytoplasmic transfer of the mtDNA nt 8993 T→G (ATP6) point mutation associated with Leigh syndrome into mtDNA-less cells demonstrates cosegregation with a decrease in state III respiration and ADP/O ratio. Proc. Natl. Acad. Sci. USA **91:** 8334–8338.
10. JIANG, S., J. CAI, D.C. WALLACE & D.P. JONES. 1999. Cytochrome c-mediated apoptosis in cells lacking mitochondrial DNA. J. Biol. Chem. **274:** 29905–29911.

11. YEN, H.C., C.Y. NIEN, H.J. MAJIMA, *et al.* 2003. Increase of lipid peroxidation by cisplatin in WI38 cells but not in SV40-transformed WI38 cells. J. Biochem. Mol. Toxicol. **17:** 39–46.
12. FRESHNEY, R.I. 2000. Culture of Animal Cells. A Manual of Basic Technique. 4th edit. John Wiley & Sons. New York.
13. CAI, J., D.C. WALLACE, B. ZHIVOTOVSKY & D.P. JONES. 2000. Separation of cytochrome c-dependent caspase activation from thiol-disulfide redox change in cells lacking mitochondrial DNA. Free Radic. Biol. Med. **29:** 334–342.
14. KIM, J., Y.H. KIM, Y. CHANG, *et al.* 2002. Resistance of mitochondrial DNA-deficient cells to TRAIL: role of Bax in TRAIL-induced apoptosis. Oncogene **21:** 3139–3148.
15. LIANG, B.C. & E. ULLYATT. 1998. Increased sensitivity to cis-diamminedichloroplatinum induced apoptosis with mitochondrial DNA depletion. Cell Death Differ. **5:** 694–701.
16. SCHONHOFF, C.M., B. GASTON & J.B. MANNICK. 2003. Nitrosylation of cytochrome c during apoptosis. J. Biol. Chem. **278:** 18265–18270.
17. HENKELS, K.M. & J.J. TURCHI. 1999. Cisplatin-induced apoptosis proceeds by caspase-3-dependent and -independent pathways in cisplatin-resistant and -sensitive human ovarian cancer cell lines. Cancer Res. **59:** 3077–3083.

Available online at www.sciencedirect.com

SCIENCE DIRECT®

Free Radical Biology & Medicine 38 (2005) 950–959

www.elsevier.com/locate/freeradbiomed

Original Contribution

Levels of reactive oxygen species and primary antioxidant enzymes in WI38 versus transformed WI38 cells following bleomcyin treatment

Hsiu-Chuan Yen[a,*], Hui-Ming Chang[a], Hideyuki J. Majima[b], Fan-Yi Chen[a], Sin-Hua Li[a]

[a]*Graduate Institute of Medical Biotechnology and Department of Medical Biotechnology and Laboratory Science, Chang Gung University, Tao-Yuan 333, Taiwan*

[b]*Department of Oncology, Kagoshima University Graduate School of Medical and Dental Sciences, Kagoshima, Japan*

Received 29 July 2004; revised 30 November 2004; accepted 15 December 2004
Available online 11 January 2005

Abstract

Bleomycin (BLM) is an anticancer drug that generates reactive oxygen species (ROS) after interacting with iron and oxygen. We hypothesized that BLM could cause a different status of oxidative stress in normal versus tumor cells due to possible altered redox status and gene expression in cells following transformation. In this study, the extent of cytotoxicity, levels of ROS, and activities of antioxidant enzymes were compared between normal WI38 cells and SV40-transformed WI38 (VA13) cells following BLM treatment. Basal activities of MnSOD and catalase were lower in VA13 cells and basal ROS levels were higher in VA13 cells. Although BLM caused greater growth inhibition and apoptosis in VA13 cells, it increased ROS levels at an earlier time point in WI38 cells. Moreover, BLM treatment (100 μg/ml) had no effect on the activities of MnSOD, CuZnSOD, and catalase, but increased the activities of glutathione peroxidase (GPX) in WI38 cells after a 48-h treatment and in VA13 cells after a 24- and 48-h treatment. Northern blot analysis indicated that the increase in GPX activities was due to increased transcript levels of GPX1 but not GPX4 in both cells. Our results indicate selective induction of the GPX1 gene by BLM and different redox responses to BLM between WI38 and VA13 cells.

Keywords: Bleomycin; Reactive oxygen species; Antioxidant enzymes; Glutathione peroxidase; Transformed cells; Free radicals

Introduction

Bleomycin (BLM) is a family of glycopeptidic antibiotics that is used as an anticancer drug in clinical use but it can also cause irreversible pulmonary toxicity in humans. BLM can interact with iron ions using five of its nitrogen atoms and bind to DNA with its bithiazole ring [1]. Based on experiments performed in test tubes, it has been postulated that after binding to Fe(II), BLM further complexes with molecular oxygen and generates the "activated BLM," possibly HO_2–Fe(III)-BLM, following subsequent reduction [2]. The activated BLM complex causes DNA strand breaksby abstraction of hydrogen from the C-4 position of the deoxyribose moiety [1]. During these reactions, superoxide and hydroxyl radicals are generated [2,3]. The Fe(III)-BLM complex would exert the same effect if reducing agents or enzymes are present [1,2,4,5]. The hydroxyl radicals produced can also lead to DNA strand breaks [3,5]. Superoxide and hydrogen peroxide may reactivate BLM for damaging DNA [2,3]. On the other hand, Kanofsky showed that the Fe(III)-BLM complex catalyzed the decomposition of long-chain unsaturated fatty acids with concurrent generation of singlet oxygen [6]. Not only the generation of ROS has been detected by electron spin resonance in vitro [2,3], but also formation of oxidative DNA adducts has been detected when directly exposing

Abbreviations: BLM, bleomycin; CAT, catalase; DIG, digoxigenin; DHR, dihydrorhodamine 123; GSH, glutathione; GPX, glutathione peroxidase; LM-PCR, ligation-mediated polymerase chain reaction; MDA, malondialdehyde; MEM, minimum essential media; NAC, *N*-acetyl-L-cysteine; NBT, nitroblue tetrazolium; ROS, reactive oxygen species; SOD, superoxide dismutase; TBARS, thiobarbituric acid-reactive substance.

* Corresponding author. Graduate Institute of Medical Biotechnology, Chang Gung University, 259-Wen-Hwa 1st Road, Kwei-Shan, Tao-Yuan 333, Taiwan. Fax: +886 3 2118692.

E-mail address: yen@mail.cgu.edu.tw (H.-C. Yen).

0891-5849/$ - see front matter © 2004 Elsevier Inc. All rights reserved.
doi:10.1016/j.freeradbiomed.2004.12.022

BLM to pure DNA [7] or erythrocyte suspensions [8]. Exposure of BLM to lymphocytes and thymocytes resulted in both single and double DNA strand breaks and apoptosis [9]. However, there was no direct evidence that ROS formation was increased by BLM in live cultured cells or in vivo. Moreover, it has been indicated that lipid peroxidation was enhanced by BLM because thiobarbituric acid-reactive substance (TBARS) for the measurement of malondialdehyde (MDA) was increased in cultured cells or animal lungs after BLM treatment [10,11], but it is now known that TBARS is not a reliable marker of lipid peroxidation [12] and MDA could be produced from the base propenal from BLM-degraded DNA [5,13].

Superoxide dismutase (SOD), catalase (CAT), and glutathione peroxidase (GPX) are the primary antioxidant enzymes that can directly scavenge ROS. SOD catalyzes the dismutation of superoxide radicals to hydrogen peroxide and oxygen. Hydrogen peroxide is further detoxified by CAT and GPX. Hydrogen peroxide and lipid hydroperoxide are reduced by GPX at the expense of glutathione (GSH) [14]. The SOD family consists of cytosolic CuZnSOD (SOD1), mitochondrial MnSOD (SOD2), and extracellular ECSOD (SOD3) [15]. Five different mammalian GPX enzymes have also been identified. GPX1 and GPX4 are ubiquitous in all types of cells and they are present in both cytosol and mitochondria, but only GPX4 can repair lipid hydroperoxide esterified on phospholipids [16,17]. Gene expression or activities of those antioxidant enzymes, especially MnSOD and GPX1, have been shown to be differentially modulated by a variety of stimuli, such as ionizing radiation, cytokines, and various oxidative insults [18–24]. On the other hand, expression of some of these antioxidant enzymes could be modulated by redox-sensitive transcription factors, such as AP-1 and NF-κB [25,26].

Previous studies investigating the effects of BLM on levels of antioxidant enzymes in animal lungs showed alteration of several antioxidant enzymes with inconsistent conclusions. Elevation of GPX activities in normal lungs at several days post-treatment has been observed [10,27–29], but it has also been found that BLM decreased GPX activity in cultured lung fibroblasts [30]. However, those previous studies only measured the total activities but not the mRNA levels of specific forms of enzymes. Also only the activities of total SOD, but not CuZnSOD and MnSOD individually, were measured in those experiments.

Differences in levels of ROS, activities of antioxidant enzymes, and responses to agents producing oxidative stress between normal and tumor cells have been implicated in the roles of oxidative stress in tumorogenesis and cancer treatment [31–35]. However, comparison of cellular or molecular changes related to oxidative stress or antioxidant enzymes using different sources of normal and tumor cells in many studies may lead to inconsistent conclusions due to intrinsic individual variations. The normal human embryonic lung fibroblast cells, WI38, and the SV40-transformed WI38 cell line, VA13 cells, were from the same origin and have been widely used to examine the effects of transformation on cellular changes and responses [31,35–39]. Oberley et al. showed that the activity of MnSOD and the level of immunoreactive MnSOD protein were lower in VA13 cells compared to WI38 cells [36]. Wan and coworkers found that total glutathione levels were much higher in VA13 cells and WI38 cells were more sensitive to cytotoxicity induced by L-buthionine sulfoximine, an agent that inhibits glutathione synthesis [37]. Allen and Balin showed that glutathione concentration was increased by increased ambient oxygen tension in WI38 cells but that in SV40-transformed WI38 cells failed to response to elevated oxygen tension, although the glutathione level was higher in transformed WI38 cells at lower oxygen tensions [31]. We have also previously shown that the anticancer drug cisplatin augmented lipid peroxidation in WI38 cell but not VA13 cells [35]. However, basal levels of ROS, GPX, and CAT and responses to BLM treatment have not been compared between these two cells.

Different redox status and other characteristics between normal and tumor cells could result in differential responses to agents inducing oxidative stress. It is therefore important to compare the effects of BLM on redox status between normal and transformed cells, which would provide more insights for improvement of cancer therapy using BLM. In this study, we examined the effects of BLM on cytotoxicity, the extent of apoptosis-associated DNA fragmentation, the levels of ROS, and the levels of primary antioxidant enzymes in WI38 and VA13 cells.

Materials and methods

Cell culture

The embryonic human lung fibroblast WI38 cell (ATCC CCL 75) and its SV40-transformed subline VA13 cell (ATCC CCL 75.1) were obtained from Riken Cell Bank, Japan. The passage number of WI38 cells used in this study was 28–34. Both cells were maintained in minimum essential media (MEM) with Earl's salts supplemented with 10% defined fetal bovine serum. Cells were cultured in a humidified atmosphere of 5% CO_2 and 95% air at 37°C.

Cytotoxicity assay

The 15-mg potency of bleomycin hydrochloride in individual ampoules was purchased from Nippon Kayaku Co. (Tokyo, Japan). Cytotoxicity was evaluated by the inhibition of cell growth or reduction of cell viability. Cells grown in 96-well tissue culture plates were treated with various doses of BLM for 48 h and were incubated with the reagent in the CellTiter 96 AQueous One solution cell proliferation assay kit (Promega, WI). The absorbance of reduced tetrazolium compound derived from the reagent due to dehydrogenase activities in viable cells was recorded at